JACS
JOURNAL OF THE AMERICAN CHEMICAL SOCIETY

COMMUNICATION

pubs.acs.org/JACS

Light-Emitting Conjugated Polymers with Microporous Network Architecture: Interweaving Scaffold Promotes Electronic Conjugation, Facilitates Exciton Migration, and Improves Luminescence

Yanhong Xu,[†] Long Chen,[†,§] Zhaoqi Guo,[†] Atsushi Nagai,[†] and Donglin Jiang*[,†,‡]

[†]Department of Materials Molecular Science, Institute for Molecular Science, National Institute of Natural Sciences, 5-1 Higashiyama, Myodaiji, Okazaki 444-8787, Japan

[‡]PRESTO, Japan Science and Technology Agency, Chiyoda-ku, Tokyo 102-0075, Japan

Supporting Information

ABSTRACT: Herein we report a strategy for the design of highly luminescent conjugated polymers by restricting rotation of the polymer building blocks through a microporous network architecture. We demonstrate this concept using tetraphenylethene (TPE) as a building block to construct a light-emitting conjugated microporous polymer. The interlocked network successfully restricted the rotation of the phenyl units, which are the major cause of fluorescence deactivation in TPE, thus providing intrinsic luminescence activity for the polymers. We show positive "CMP effects" that the network promotes π-conjugation, facilitates exciton migration, and improves luminescence activity. Although the monomer and linear polymer analogue in solvents are nonemissive, the network polymers are highly luminescent in various solvents and the solid state. Because emission losses due to rotation are ubiquitous among small chromophores, this strategy can be generalized for the de novo design of light-emitting materials by integrating the chromophores into an interlocked network architecture.

Conjugated polymers play a vital role in lasing, light-emitting diodes, flexible transistors, and solar cells. Owing to their rigid conformation, they have a high tendency to aggregate in solution and the solid state. Such aggregation leads to the dissipation of excitation energy and ultimately limits their utility as light-emitting motifs. To resolve this issue, molecular approaches based on site isolations with bulky polymeric matrices have been developed to prevent the aggregation of conjugated polymers. These approaches provide highly luminescent polymers, but at the price of a loss in interchain electronic communications.[1]

Herein we report a new strategy for the construction of light-emitting conjugated polymers based on conjugated microporous architectures.[2−5] We employed tetrakis(4-bromophenyl)ethene (TPTBE) as a single component for the synthesis of a new conjugated microporous polymer (TPE-CMP), in which the TPE units are directly linked to form an interlocked network (Chart 1A). TPE is a typical aggregation-induced emission chromophore in that rotation of the peripheral phenyl groups leads to a decay in the excitation energy and reduces the luminescence activity.[6] Direct interweaving of TPE into a network structure restricts the rotation of the phenyl groups, thus providing the network with high luminescence activity. We demonstrate that the network structure promoted electronic conjugation, facilitated exciton migration, and enhanced luminescence activity. In sharp contrast to the monomer and linear polymer analogues, which are almost nonemissive in solutions, the network polymers are highly luminescent in both solution and the solid state. This result is also distinct from conventional conjugated polymers, which generally lose their luminescence properties in the solid state. In contrast to the site isolation approach, the porous network strategy is unique in that it not only enhances luminescence but also promotes π-electronic interactions via the conjugated network scaffolds.

Chart 1. (A) Schematic Representation of Linear TPE-LP and Synthesis of TPE-CMP; (B) Closed Tetragonal Skeleton and (C) Open Framework of the TPE-CMP Segments Simulated by DFT Calculations at the B3LYP 6-31G* Level (phenyl, blue; ethene, yellow; H, white)

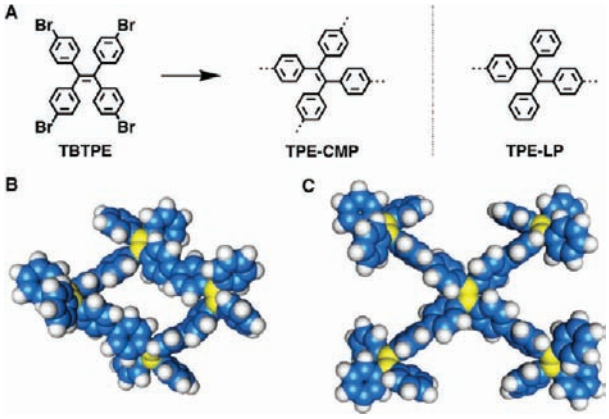

TBTPE was used as a monomer in a Yamamoto coupling reaction to develop the CMP network (Supporting Information (SI)). The TPE-CMP samples were unambiguously characterized by elemental and infrared analysis and solid-state ^{13}C cross-polarization magic angle spinning NMR spectroscopy (SI Figures S1 and S2). To monitor the development of the porous network and the growth in π-conjugation, time-dependent Yamamoto reactions were conducted. The Yamamoto reactions were thus carried out at 2, 12, 36, and 72 h to produce TPE-CMP@2h, TPE-CMP@12h, TPE-CMP@36h, and TPE-CMP@72h, respectively (SI). TPE-CMP is amorphous without crystallinity as evidenced by X-ray

Received: September 2, 2011
Published: October 06, 2011

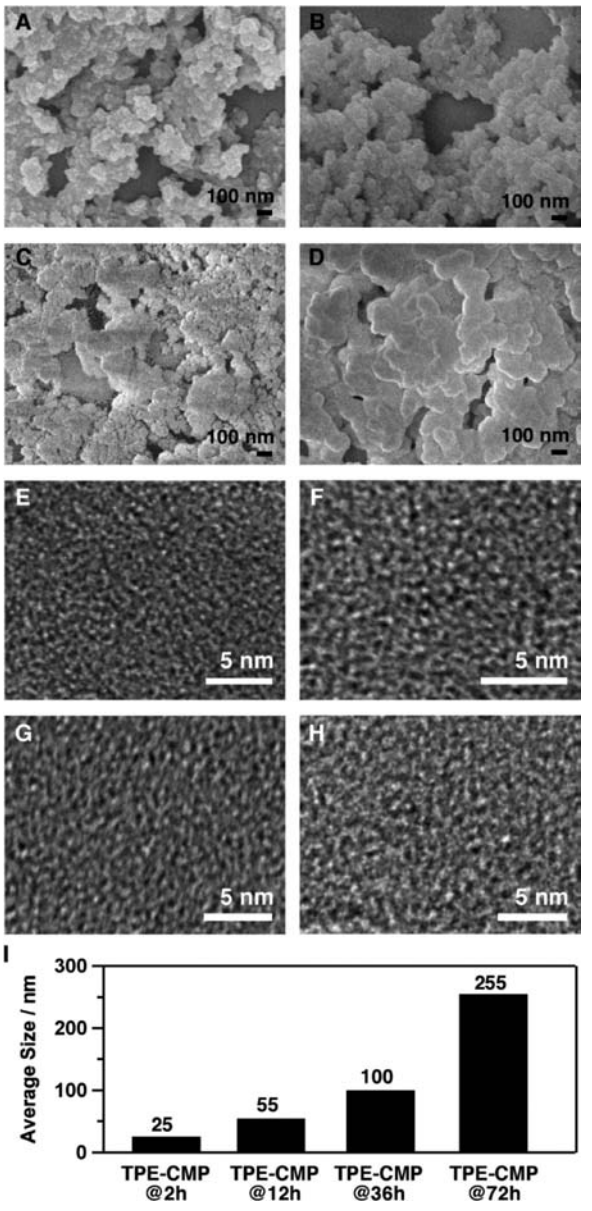

Figure 1. FE-SEM images of the TPE-CMP samples synthesized over 2 (A), 12 (B), 36 (C), and 72 h (D). HR-TEM images of the TPE-CMP samples synthesized over 2 (E), 12 (F), 36 (G), and 72 h (H). (I) Average size of TPE-CMP platelets synthesized over different reaction times.

diffraction analysis (SI Figure S3). Field emission scanning electron microscopy (FE-SEM) revealed that TPE-CMP consists of platelet-like particles, the size of which increased with reaction time (Figure 1A–D). For example, the average size was about 25 nm after 2 h reaction, which was increased to 55, 100, and further to 255 nm when the reaction time was extended to 12, 36, and then to 72 h (Figure 1I). Interestingly, the microporous structure can be directly visualized by high resolution tunneling electron microscopy (HR-TEM) (Figures 1E–H). One clear feature of the porous textures is that the micropores are present homogenously and are similar in size regardless of the reaction time.

Nitrogen sorption isotherm measurements at 77 K were performed to characterize their pore structures. All of the TPE-CMP samples gave reversible curves with microporous characteristics, regardless of reaction time (Figure 2A–D).

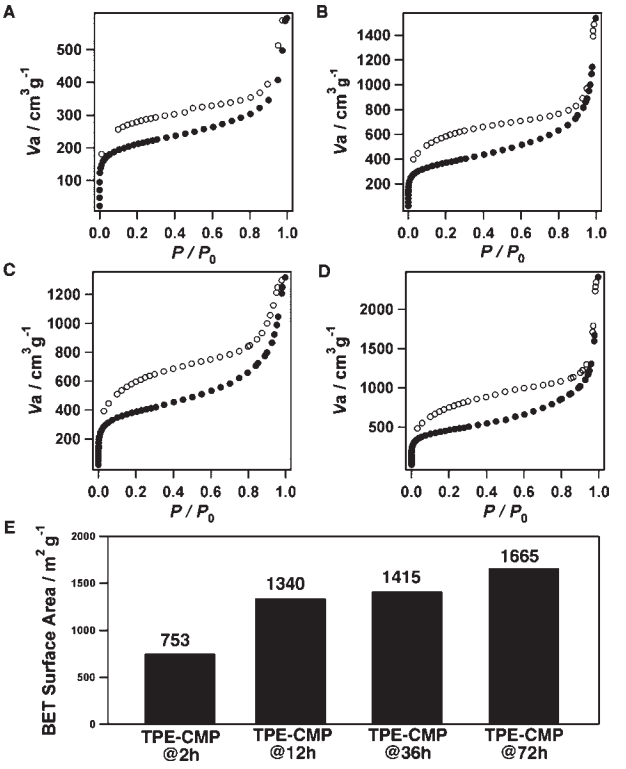

Figure 2. Nitrogen sorption isotherm curves of TPE-CMP synthesized over 2 (A), 12 (B), 36 (C), and 72 h (D). (E) BET surface areas of the TPE-CMP samples synthesized over different reaction times.

The Brunauer–Emmett–Teller (BET) surface area increased with increasing reaction time. For example, the BET surface area of the TPE-CMP@2h sample is 753 $m^2\ g^{-1}$, which increases sharply to 1340 $m^2\ g^{-1}$ for the TPE-CMP@12h sample before reaching 1665 $m^2\ g^{-1}$ after reaction for 72 h (Figure 2E). Pore size distribution profiles reveal the presence of micropores with a size of about 0.8 nm, with similar distributions for the samples synthesized over different reaction times (SI Figure S4). These results suggest that the TPE-CMP network grows larger with increasing reaction time to achieve large surface area but with retained pore size.

To obtain an insight into the network structure, we performed semi-empirical calculations using the Gaussian 03 program at the PM3 level and then at the B3LYP/6-31G level with a hybrid density functional theory (DFT) method.[7] We calculated two typical frameworks for the TPE-CMP structure. Calculations of an elementary closed tetragon gave a pore width of 0.8 nm (Chart 1B), which is consistent with the size of the micropores in the actual TPE-CMP structure. On the other hand, the five-member framework shows significant twisting at the peripheral TPE units and their distortion eventually leads to the growth of the CMP skeleton into an amorphous, three-dimensional network morphology (Chart 1C). It is clear that the porosity is permanent by virtue of the interweaving nature of the network.

The network skeleton allows a progressed extension of π-electronic conjugation. For example, TBTPE exhibited an absorption band at 316 nm (Figure 3A, dotted black curve). In sharp contrast, the TPE-CMP@2h sample showed an absorption band at 342 nm (blue curve), which is red-shifted by 26 nm from that of TBTPE. When the reaction time was increased, the absorption band was further red-shifted to 356, 358, and 368 nm for the TPE-CMP@12h, TPE-CMP@36h, and TPE-CMP@72h samples,

dx.doi.org/10.1021/ja208284t |J. Am. Chem. Soc. 2011, 133, 17622–17625

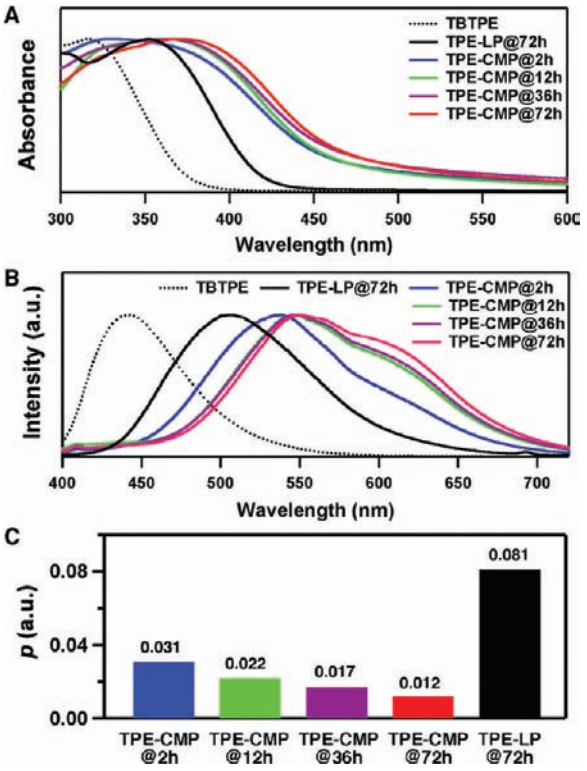

Figure 3. (A) Normalized electronic absorption and (B) fluorescence spectra of TPE-CMP, TBTPE, and TPE-LP in THF at 25 °C. (C) Fluorescence depolarization p of TPE-CMP and TPE-LP.

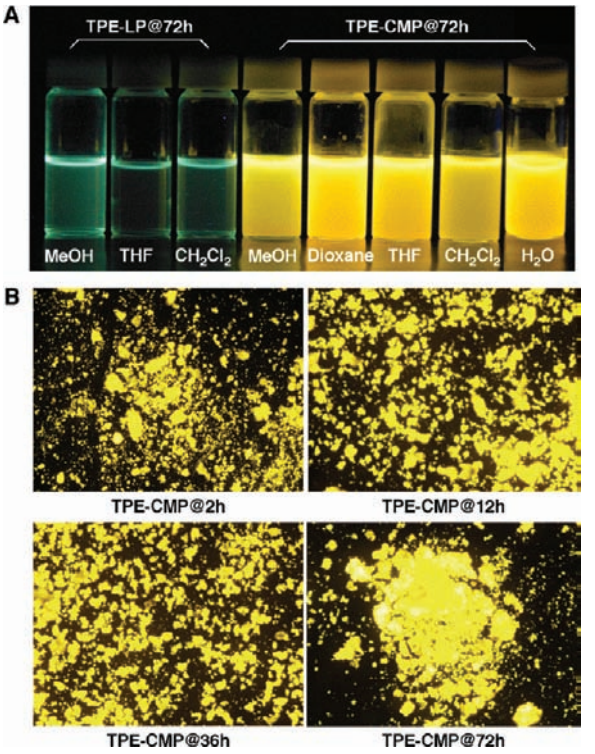

Figure 4. (A) Photos of TPE-LP@72 h in MeOH, THF, and CH_2Cl_2 and TPE-CMP@72 h in MeOH, dioxane, THF, CH_2Cl_2, and water, under a handy UV light. (B) Fluorescence microscopic images of TPE-CMP synthesized over different reaction time.

respectively. The observed red-shifts of the absorption bands of the TPE-CMP samples indicate the extension of electronic conjugation over the CMP skeletons. In contrast, under identical conditions, a linear polymer synthesized over 72 h (TPE-LP@72h) exhibited an absorption band at only 352 nm (black curve).

Upon excitation at 316 nm, the TBTPE monomer in THF at 25 °C emitted very weakly at 443 nm (Figure 3B, dotted black curve). In contrast, the TPE-CMP@2h sample emits strong luminescence at 538 nm (blue curve) upon excitation at 342 nm. Again, the emission bands of the TPE-CMP@12h (green curve), TPE-CMP@36h (purple curve), and TPE-CMP@72h (red curve) samples were increasingly red-shifted to 545, 547, and 551 nm, respectively (Figure 3B), indicating extended π-electronic conjugation over the CMP skeleton. In contrast, the linear polymer TPE-LP@72h gave only very weak luminescence at a much shorter wavelength of 506 nm (black curve). Because the similarity between the fluorescence spectra in the solid state and solutions, the small shoulder of TPE-CMPs is likely related to an intra-network chromophore interaction other than inter-network process.

Since the network allows for extended electronic conjugation, we investigated the fluorescence depolarization profiles of the TPE-CMP samples, which are considered to reflect the occurrence of photochemical events in the microporous network. Suppression of Brownian motion in a viscous medium should result in fluorescence depolarization occurring predominantly by exciton migration along the conjugated chain. Here, the degree of fluorescence depolarization (p) is defined as $p = (I_{\parallel} - GI_{\perp})/(I_{\parallel} + GI_{\perp})$, where $I_{\parallel}$ and $I_{\perp}$ are the fluorescence intensities of the parallel and perpendicular components relative to the polarity of the excitation light, respectively, while G is an instrumental correction factor. Excitation at the absorption maxima of viscous solutions of the TPE-CMP samples in polyethylene glycol at 25 °C gave fluorescence depolarization profiles (Figure 3C), in which the value of p became smaller as the reaction time increased. For example, the p value for the TPE-CMP@2h sample was 0.031, which dropped to 0.017 and further to 0.012 when the reaction time was increased to 36 h (TPE-CMP@36h) and then to 72 h (TPE-CMP@72h). In contrast, the linear polymer TPE-LP@72h exhibited a much higher p value of 0.081. The absence of saturation in this effect even for the TPE-CMP@72h sample is quite interesting, since previous studies on linear conjugated polymers have shown that the exciton migration subsides within several nanometers. Therefore, the CMP structure is considered to be significantly different from the linear chain structure, facilitating exciton migration over the three-dimensional network.

The absolute quantum yield of fluorescence (Φ_{FL}) of TPE-CMP in THF at 25 °C was evaluated using an integrating sphere method. The Φ_{FL} values of TBTPE and TPE were only 0.16% and 0.20%, respectively. Similarly, TPE-LP@72h exhibited a Φ_{FL} value of only 0.65%. In sharp contrast, the Φ_{FL} value of TPE-CMP@2h was as high as 40% under identical condition. Interestingly, all the TPE-CMP samples exhibited similarly high Φ_{FL} values. As control experiments, we further investigated the luminescence of TPE and TPE-LP@72h in their aggregated states to show the effects of aggregation-induced emission. Adding water to their THF solutions leads to the formation of aggregates, which displayed the maxima Φ_{FL} values of only 14% and 22%, respectively. Therefore, these encouraging results indicate that the interwoven CMP scaffold can efficiently enhance luminescence activity.

Because the network is interlocked, the TPE-CMP samples retain their luminescence activity, irrespective of the solvent

dx.doi.org/10.1021/ja208284t |J. Am. Chem. Soc. 2011, 133, 17622–17625

(SI Figure S5). For example, the TPE-CMP@72h sample exhibited high luminescence in various solvents such as MeOH, dioxane, THF, CH_2Cl_2, $CHCl_3$, hexane, DMF, benzene, and water (Figure 4A and S5). In sharp contrast, the linear analogue TPE-LP@72h is almost nonemissive in CH_2Cl_2, $CHCl_3$, and THF (Figure 4A). In solvents such as MeOH, which causes chain aggregation and suppresses rotation of the phenyl units, TPE-LP@72h became weakly luminescent (Figure 4A). More significantly, the TPE-CMP samples are highly luminescent even in the solid state, without showing deterioration in light-emitting activity or with any differences apparent between the samples prepared over different reaction time (Figure 4B).

Taking all the above results into account, it is likely that the TPE-CMP network acts to suppress the rotation of the phenyl units, which is desirable for electronic conjugation, may also preserve the fluorescence anisotropy, and allows long-range exciton migration (Figure 3C). Several examples of luminescent TPE derivatives have been reported in which solvent-induced aggregation is considered to restrict the rotation of the phenyl units.[6] We assume that a network structure could similarly limit the rotation of the phenyl units, because each TPE unit is effectively interlocked by covalent bonds from four different directions. The similarly high Φ_{FL} values for the TPE-CMP samples synthesized over different reaction time indicate the effectiveness in suppressing the phenyl rotation. Such conformational confinement of the TPE units in the network may promote conjugation and facilitate exciton migration. On the other hand, in the linear TPE-LP, two freely rotatable phenyl groups remain for each TPE repeating unit, which accounts for the low luminescence activity. Therefore, unlike the small TPE molecules and its linear polymer analogues, which require external conditions such as aggregation to temporarily "stabilize" their fluorescence, the TPE-CMP structure suppresses the rotation of the phenyl units by virtue of its interwoven network, thus providing intrinsic luminescent activity.

In summary, we have described a strategy for the synthesis of a highly luminescent conjugated polymer based on a conjugated microporous architecture. The CMP network with three-dimensionally interlocked skeleton suppresses the rotation of building blocks, promotes π-electronic conjugation, facilitates exciton migration, and enhances luminescence irrespective of the solvent and material state. These positive "CMP effects" on π-electronic conjugation feature CMPs as a unique platform for the design of de novo conjugated materials, which can be difficult to achieve with conventional linear polymers. Because emission losses induced by rotation are ubiquitous among chromophores, this network approach can be generalized for the development of various efficient light emitters and wavelength converters.

■ ASSOCIATED CONTENT

Supporting Information. Complete ref 7, detailed experimental procedures, FTIR and NMR spectra, and XRD and pore distribution profiles. This material is available free of charge via the Internet at http://pubs.acs.org.

■ AUTHOR INFORMATION

Corresponding Author
jiang@ims.ac.jp

Present Addresses
[§]Max Planck Institute for Polymer Research.

■ ACKNOWLEDGMENT

We are grateful for financial support from PRESTO, JST. The computations were performed using Research Center for Computational Science, Okazaki, Japan. This work was supported by NSFC (Grant No. 21128001).

■ REFERENCES

(1) (a) Hecht, S.; Fréchet, J. M. J. *Angew. Chem., Int. Ed.* **2001**, *40*, 74–91. (b) Sato, T.; Jiang, D.-L; Aida, T. *J. Am. Chem. Soc.* **1999**, *121*, 10658–10659. (c) Jiang, D.-L.; Choi, C.-K.; Honda, K.; Li, W.-S.; Yuzawa, T.; Aida, T. *J. Am. Chem. Soc.* **2004**, *126*, 12084–12089. (d) Li, W.-S.; Jiang, D.-L.; Aida, T. *Angew. Chem., Int. Ed.* **2004**, *43*, 2943–2947.

(2) (a) Cooper, A. I. *Adv. Mater.* **2009**, *21*, 1291–1295. (b) Thomas, A.; Kuhn, P.; Weber, J.; Titirici, M. M.; Antonietti, M. *Macromol. Rapid Commun.* **2009**, *30*, 221–236.

(3) (a) Jiang, J. X.; Su, F.; Trewin, A.; Wood, C. D.; Campbell, N. L.; Niu, H.; Dickinson, C.; Ganin, A. Y.; Rosseinsky, M. J.; Khimyak, Y. Z.; Cooper, A. I. *Angew. Chem., Int. Ed.* **2007**, *46*, 8574–8578. (b) Jiang, J. X.; Su, F.; Trewin, A.; Wood, C. D.; Niu, H.; Jones, J. T. A.; Khimyak, Y. Z.; Cooper, A. I. *J. Am. Chem. Soc.* **2008**, *130*, 7710–7720. (c) Jiang, J. X.; Su, F. B.; Niu, H. J.; Wood, C. D.; Campbell, N. L.; Khimyak, Y. Z.; Cooper, A. I. *Chem. Commun.* **2008**, 486–488. (d) Stöckel, E.; Wu, X. F.; Trewin, A.; Wood, C. D.; Clowes, R.; Campbell, N. L.; Jones, J. T. A.; Khimyak, Y. Z.; Adams, D. J.; Cooper, A. I. *Chem. Commun.* **2009**, 212–214. (e) Jones, J. T. A.; Holden, D.; Mitra, T.; Hasell, T.; Adams, D. J.; Jelfs, K. E.; Trewin, A.; Willock, D. J.; Day, G. M.; Bacsa, J.; Steiner, A.; Cooper, A. I. *Angew. Chem., Int. Ed.* **2011**, *50*, 749–753. (f) Dawson, R.; Laybourn, A.; Clowes, R.; Khimyak, Y. Z.; Adams, D. J.; Cooper, A. I. *Macromolecules* **2009**, *42*, 8809–8816. (g) Hasell, T.; Wood, C. D.; Clowes, R.; Jones, J. T. A.; Khimyak, Y. Z.; Adams, D. J.; Cooper, A. I. *Chem. Mater.* **2010**, *22*, 557–564. (h) Jiang, J. X.; Wang, C.; Laybourn, A.; Hasell, T.; Clowes, R.; Khimyak, Y. Z.; Xiao, J. L.; Higgins, S. J.; Adams, D. J.; Cooper, A. I. *Angew. Chem., Int. Ed.* **2011**, *50*, 1072–1075. (i) Jiang, J.-X.; Trewin, A.; Adams, D. J.; Cooper, A. I. *Chem. Sci.* **2011**, *2*, 1777–1781.

(4) (a) Bojdys, M. J.; Wohlgemuth, S. A.; Thomas, A.; Antonietti, M. *Macromolecules* **2010**, *43*, 6639–6645. (b) Schmidt, J.; Weber, J.; Epping, J. D.; Antonietti, M.; Thomas, A. *Adv. Mater.* **2009**, *21*, 702–705. (c) Wang, X. C.; Maeda, K.; Thomas, A.; Takanabe, K.; Xin, G.; Carlsson, J. M.; Domen, K.; Antonietti, M. *Nat. Mater.* **2009**, *8*, 76–80. (d) Palkovits, R.; Antonietti, M.; Kuhn, P.; Thomas, A.; Schüth, F. *Angew. Chem., Int. Ed.* **2009**, *48*, 6909–6912. (e) Wang, X. C.; Chen, X. F.; Thomas, A.; Fu, X. Z.; Antonietti, M. *Adv. Mater.* **2009**, *21*, 1609–1612.

(5) (a) Chen, L.; Yang, Y.; Jiang, D. *J. Am. Chem. Soc.* **2010**, *132*, 9138–9143. (b) Chen, L.; Yang, Y.; Guo, Z.; Jiang, D. *Adv. Mater.* **2011**, *23*, 3149–3154. (c) Chen, L.; Honsho, Y.; Seki, S.; Jiang, D. *J. Am. Chem. Soc.* **2010**, *132*, 6742–6748. (d) Kou, Y.; Xu, Y.; Guo, Z.; Jiang, D. *Angew. Chem., Int. Ed.* **2011**, *50*, 8753–8757.

(6) (a) Zhao, Z.; Chen, S.; Shen, X.; Mahtab, F.; Yu, Y.; Lu, P.; Lam, J. W. Y.; Kwoka, H. S.; Tang, B. Z. *Chem. Commun.* **2010**, *46*, 686–688. (b) Vyas, V. S.; Rathore, R. *Chem. Commun.* **2010**, *46*, 1065–1067. (c) Chen, Q.; Bian, N.; Cao, C.; Qiu, X. L.; Qib, A.; Han, B. H. *Chem. Commun.* **2010**, *46*, 4067–4069. (d) Zhao, Z. J.; Chen, S. N.; Lam, J. W. Y.; Jim, C. K. W.; Chan, C.Y. K.; Wang, Z. M.; Lu, P.; Deng, C. M.; Kwok, H. S.; Ma, Y. G.; Tang, B. Z. *J. Phys. Chem. C* **2010**, *114*, 7963–7972. (e) Wang, M.; Zhang, G.; Zhang, D.; Zhu, D.; Tang, B. Z. *J. Mater. Chem.* **2010**, *20*, 1858–1867. (f) Wang, W. Z.; Lin, T. T.; Wang, M.; Liu, T. X.; Ren, L. L.; Chen, D.; Huang, S. *J. Phys. Chem. B* **2010**, *114*, 5983–5988. (g) Yuan, W. Z.; Zhao, H.; Shen, X. Y.; Mahtab, F.; Lam, J. W. Y.; Sun, J. Z.; Tang, B. Z. *Macromolecules* **2009**, *42*, 9400–9411. (h) Wang, M.; Gu, X. G.; Zhang, G. X.; Zhang, D. Q.; Zhu, D. B. *Anal. Chem.* **2009**, *81*, 4444–4449. (i) Liu, L.; Zhang, G. X.; Xiang, J. F.; Zhang, D. Q.; Zhu, D. B. *Org. Lett.* **2008**, *10*, 4581–4584. (j) Tong, H.; Hong, Y.; Dong, Y.; Häußler, M.; Lam, J.W. Y.; Li, Z.; Guo, Z.; Guo, Z.; Tang, B. Z. *Chem. Commun.* **2006**, 3705–3707. (k) Chen, Q.; Wang, J. X.; Yang, F.; Zhou, D.; Bian, N.; Zhang, X. J.; Yan, C. G.; Han, B. H. *J. Mater. Chem.* **2011**, *21*, 13554–13560. (l) Patra, A.; Koenen, J.-M.; Scherf, U. *Chem. Commun.* **2011**, *47*, 9612–9614.

(7) Frisch, M. J.; et al. *Gaussian 03*, revision E.01; Gaussian, Inc.: Wallingford, CT, 2004.